Propagation Errors and Scintillation on Trans - Ionospheric Links

Y. Béniguel
IEEA, 13, Promenade Paul Doumer, 92400 Courbevoie, France
beniguel@ieea.fr

Abstract

Signal scintillation due to propagation through a turbulent ionosphere may cause strong modifications of transmitted signals. This can be essentially observed at low latitudes (from – 20° to +20°) and at high latitudes. The low latitudes region is the most affected and the scintillation level is related to the solar activity. The calculation of the transmitted field allows estimating signal impairments, in particular its intensity and phase fluctuations. The Mutual Coherence Function characterizes the channel transfer function. It is required for radar performances assessment after propagation through the turbulent medium. It has been shown that under simplified hypothesis, an analytical solution can be derived allowing a sensitivity analysis study.

1. Introduction

As a result of propagation through ionosphere electron density irregularities, transionospheric radio signals may experience amplitude and phase fluctuations. In equatorial regions, these signal fluctuations specially occur during equinoxes, after sunset, and last a few hours. They are more intense in periods of high solar activity. There is also a longitudinal dependency. Scintillations are more common in South America near the December solstice than at the equinoxes. These fluctuations result in signal degradation from VHF up to C band. They are a major issue for many systems including Global Navigation Satellite Systems (GNSS), telecommunications, remote sensing and earth observation,.

The signal fluctuations, referred as scintillations, are created by random fluctuations of the medium's refractive index, which are caused by inhomogeneities inside the ionosphere. These inhomogeneities are sub structures of bubbles which may reach dimensions of several hundreds of kilometers as can be seen from radar observations [1]. These bubbles present a patchy structure. They appear after sunset when the sun ionization drops to zero. Instability processes develop inside these bubbles with creation of turbulences inside the medium. The propagation through these turbulences creates scintillation.

This paper will present the results obtained with a model named Global Ionospheric Scintillation Model (GISM) [2], aiming to reproduce the effects of propagation through this medium, namely the intensity and phase fluctuations of the transmitted signal and the Mutual Coherence Function (MCF) of interest for radar applications. Comparisons of results obtained with measurements are presented.

2. Scattered field calculation

2.1 Theoretical formulation

The wave propagation is calculated solving the Helmholtz equation [3].

$$\left[\nabla^2 + k^2 \left(1 + \varepsilon_1(\bar{r})\right)\right] u(\bar{r}, z) = 0 \qquad (1)$$

Where

- $k^2 = \omega^2 \mu_0 \varepsilon_0 \langle \varepsilon_r \rangle = k_0^2 \langle \varepsilon_r \rangle$ is the local wave number
- μ_0, ε_0 and k_0 are the free space permeability, permittivity and wave number
- $\bar{r}$ is one observation point inside the medium and z is the coordinate along the direction of propagation.

The dielectric permittivity along the main propagation axis *z*, is written:

$$\varepsilon_r(\bar{r}) = \langle \varepsilon_r \rangle \left[1 + \varepsilon_1(\bar{r})\right] \qquad (2)$$

with $\varepsilon_1(\bar{r})$ is the random part of the relative dielectric permittivity.

Introducing the complex amplitude $U(\bar{r}, z)$ of the stochastic field and assuming that the variation of the

978-88-907018-1-8/13/$31.00 ©2013 IEEE

complex amplitude is mainly in the direction perpendicular to the main propagation axis (parabolic approximation), the stochastic parabolic equation for the complex amplitude can be written in the form

$$2jk\frac{\partial U(\bar{r},z)}{\partial z}+\nabla_t^2 U(\bar{r},z)+k^2\varepsilon_1(\bar{r},z)\,U(\bar{r},z)=0 \qquad (3)$$

where ∇_t^2 is the transverse Laplacian.

2.2 Algorithm

To solve this equation, the medium is divided into a series of successive layers (or screens) perpendicular to the main propagation axis, each one being characterized by local homogeneous statistical properties. The solution is then obtained by iterating successively scattering and propagation calculations.

The first calculation uses the first and third term of (3). It describes the phase change due to the presence of random fluctuations $\varepsilon_1(r,z)$; r is the distance to the propagation direction main axis.

$$2jk\frac{\partial U(r,z)}{\partial z}+k^2\varepsilon_1(r,z)\,U(r,z)=0 \qquad (4)$$

with solution

$$U(r,z+\Delta z)=U(r,z)\exp\left(jk\,\Delta z\,\varepsilon_1(r,z)/2\right) \qquad (5)$$

The second equation describes propagation between two screens. It uses the first and second term of (3).

$$2jk\frac{\partial U(r,z)}{\partial z}+\nabla^2 U(r,z)=0 \qquad (6)$$

It is solved using an FFT technique. Applying this two steps technique to each successive layer, the multiple phase screens (MPS) solution of the parabolic equation is obtained.

2.3 Phase synthesis on a phase screen

In the MPS technique, successive planes perpendicular to the direction of propagation are considered. On each one of these planes, a phase synthesis shall be performed. In general, the medium's power spectral density of phase fluctuations can be approximated by expression:

$$\gamma_\Phi(k)=\frac{C_P}{\left(k^2+q_0^2\right)^{p/2}} \qquad (7)$$

Where

- Cp characterizes the turbulence strength. It is related to the variance of the electron density.
- $q_0=2\pi/L_0$ and L_0 is the outer scale of the inhomogeneities.
- p is the spectrum slope. The spectrum is consequently linear using Log - Log scales.
- The variables k and r are corresponding variables in the Fourier transform.

The ionosphere inhomogeneities develop in a plane perpendicular to the terrestrial magnetic field and may be considered as ellipsoids with main axis aligned with the terrestrial magnetic field. The dimensions of these structures may reach hundreds of km and the medium is consequently anisotropic.

Using an appropriate change of variables [4], and correspondingly including a geometrical factor, the calculation can still be done using a 2D geometry (1D phase screens). The axis reference system contains the direction of propagation (the Line Of Sight) and the terrestrial magnetic field vector.

2.4 Results obtained

Inputs of the model are the transmitter and receiver locations, the time, day and year of observation, and the geophysical parameters. Based on the PRIS measurements campaign [5], experimental laws have been derived for the geographic and local time dependency. As mentioned previously the spectrum is characterized by three parameters: the slope, a typical dimension of inhomogeneities and the strength. Default values are respectively set to p = 3, L_0 = 1 kilometre and $\sigma_{Ne}=0.1\langle N_e\rangle$. As geophysical parameters, only the average 10.7 cm solar flux number is considered. Its value is taken from the curves published by the National Oceanic and Atmospheric Administration (www.noaa.gov).

For earth space links, the source point is the antenna onboard the satellite and the observation point is on the ground. Once the line of sight is determined, phase screens are set along this line and statistical parameters are associated to each one of these screens. The algorithm provides the field $U(r)$ at the observation point, where r is the dimension transverse to the direction of propagation. Dependency of the received field on the time can be obtained, considering both the source displacement and the medium drift velocity. A time series of the received field is obtained in that case.

GISM calculates a mean value of the scintillation indices both for intensity and phase fluctuations. The fluctuating medium is assumed to be statistically homogeneous. The reality is different to some extent. The medium has a patchy structure and links meeting the geographic and time conditions may not be affected due to this patchy structure. Consequently a probability of occurrence should be given together with the mean value. This is not provided in the current version of the model. The corresponding

probability shall be obtained from a measurements analysis.

Two indices are defined to characterize the scintillations: the standard deviation of the normalized intensity, named S4, and the phase standard deviation. The scintillation event strength is defined with respect to the S4 value which is between 0 and 1. A value of 1 will correspond to about 35 dB peak to peak of intensity fluctuations. The scintillation strength is weak (S4 < 0.3), medium (0.3 < S4 < 0.6) or strong (S4 > 0.6) depending on the case. This usual classification refers to the fade levels and the resulting constraints on a navigation system, from -2 dB to + 2 dB in the weak regime up to more than 20 dB peak to peak for the strong regime.

One example of the time series provided by GISM is shown on Figure 1 for a strong fluctuation case. Similar time series are recorded by measurements. The S4 scintillation index is 0.9 in that case.

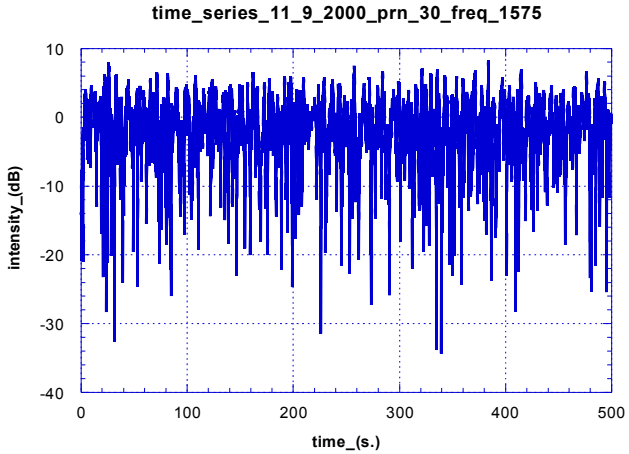

Figure 1: Intensity time series on a strong fluctuation event (S4 = 0.9)

2.5 Comparison with measurements

The results reported hereafter are taken from the PRIS measurement campaign [5] carried out under ESA / ESTEC contract N° 19530. For this study, a number of receivers were deployed both at low and high latitudes, in particular in Vietnam, Indonesia, Guiana, Cameroon, Chad and Sweden. These receivers were dedicated receivers, operating at 50 Hz. A data bank was constituted and the scintillation characteristics were derived from an extensive analysis of this data bank. Comparisons between measurements and results provided by the GISM model in the same conditions were performed both for the scintillation indices and on the spectrum.

Scintillation indices

One week of measurements at Cayenne, French Guiana was selected. The results are presented in the Figures 2. The x axis corresponds to local time at receiver location. The 0 value has been set arbitrarily to Saturday 19:00, the week of observation.

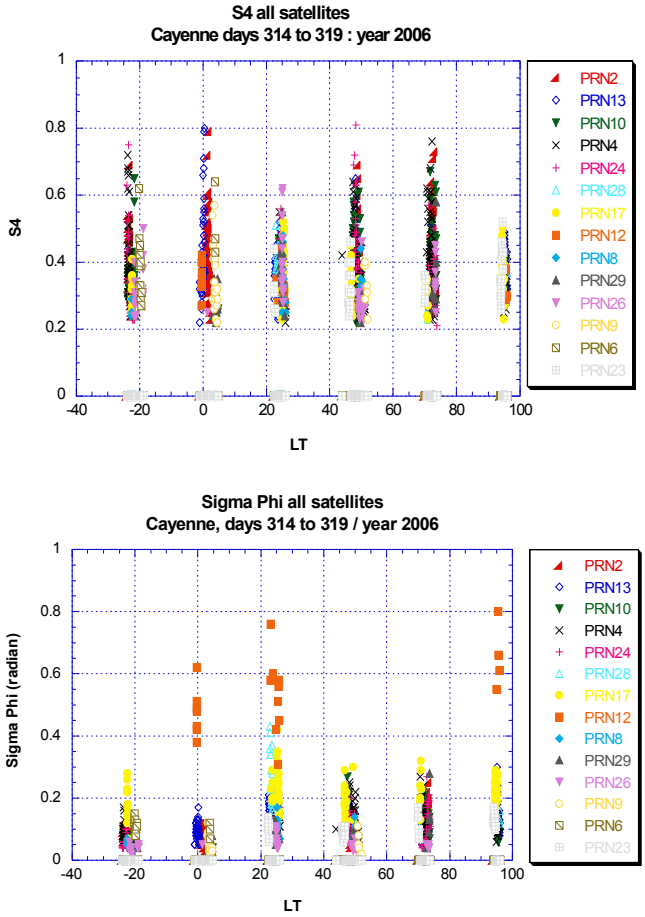

Figure 2: Intensity and phase scintillation indices measurements on GPS week N° 377

Measurements

The local time of the x axis corresponds to hours in GPS time. Each point corresponds to a 1 minute sample. Only points with a S4 value greater than 0.2 were retained in the analysis. A 5° mask elevation angle was taken when recording the data. In addition multipath is rejected using the code carrier divergence algorithm recommended in the Novatel GSV 4004 user manual. As can be seen on Figure 3, the points are clustered every evening at post sunset hours, typically 19:00 - 24:00. No average is taken on the data. The scintillation activity occurred quite regularly that week with comparable levels. The S4 average value is about 0.4. The flux number that week (GPS week N° 377, modulo 1024) was equal to 90.

The phase fluctuations are plotted concurrently. The mean value is about 0.2, consequently lower than the S4 value. This observation is quite common. A few points exhibit high values. Deep fades occur concurrently to these high values. In the case of very small values this creates phase jumps. As a consequence the phase and intensity standard deviations are no longer related.

The scintillation characteristics, both indices and spectral parameters, have been calculated using 1 minute samples. This calculation brings no particular difficulty for the intensity, which practically does not change during one minute. The calculation of the phase parameters is more difficult. A high pass 6th order filter is used to remove the low frequency components of the signal.

Modelling

The scenario was replayed using the corresponding Yuma files for one particular day of the week. The results obtained are presented on Figure 3. A different day will not bring significant differences considering that the geophysical parameters would have been quite identical. The flux number, input to GISM, was equal to approximately 90 that week. As mentioned previously, the model provides a mean value. It overestimates the number of affected links due to the fact that the probability of occurrence is not considered. Only the mean values can be compared. The scintillation intensity index mean value is about 0.4. This corresponds to the measurements. The scintillation phase index mean value is slightly greater than the one recorded in the measurements. In both cases the phase RMS is lower than the intensity RMS, and in both cases some points exhibit high values due to the phase jumps.

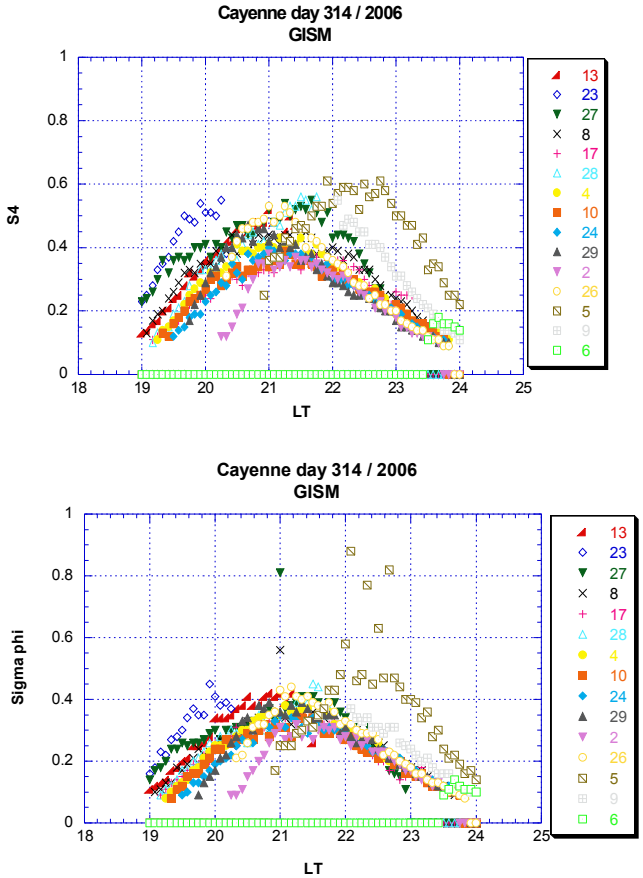

Figure 3: Intensity and phase scintillation indices on day 314, GPS week N° 377, obtained by modeling

2.6 Medium Extent

Figure 4 shows a scintillation map for vertical links. Slant observations may exhibit higher values due to a longer path inside the fluctuating medium.

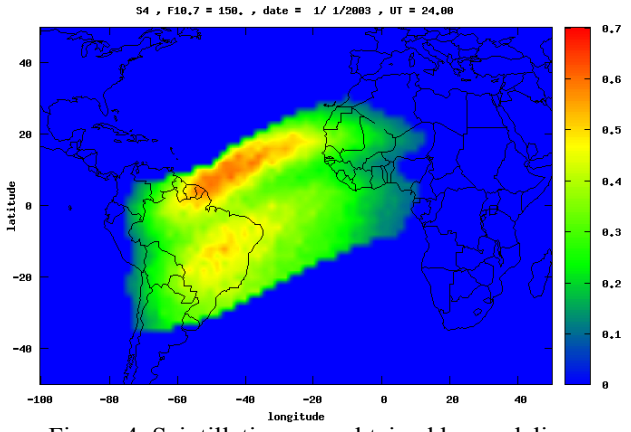

Figure 4: Scintillation map obtained by modeling

Figure 4 was obtained for an average solar radio flux at 10.7 cm set to 150. This corresponds to a high value. Universal time is 12 p.m. At this time the peak values for the TEC occur in the Pacific Ocean area. For the scintillations the time duration of the events is a few hours after sunset. The model presented here calculates the effects at the equatorial regions. The peak value for the intensity RMS (S4 parameter) is equal to 0.7 and corresponds to strong fluctuations.

3. Second order moment of the field

The previous section has shown the intensity fluctuations which are a major concern for telecommunications and navigation applications. For a radar application, the coherence properties of the transmitted field are required. The mutual coherence function (MCF), noted Γ, characterizes the coherence properties of the transmitted field. With respect to the transmitted field, Γ is the following function:

$$\Gamma(z,k_1,k_2,r_1,r_2) = \left\langle U_1(z,k_1,r_1)\ U_2^*(z,k_2,r_2) \right\rangle \quad (8)$$

It is calculated using the wave propagation equation, written for two frequencies and two positions and then combining the equations obtained [3]. Γ is a solution of equation:

$$\left[2j\frac{\partial}{\partial z} + \frac{1}{k_1}\nabla_{t1}^2 - \frac{1}{k_2}\nabla_{t2}^2 + \frac{jk_p^4}{4}\left[\left(\frac{1}{k_1^2}+\frac{1}{k_2^2}\right)A_\xi(0) - \frac{2}{k_1k_2}A_\xi(\rho)\right]\right]\Gamma(z,\rho) = 0 \quad (9)$$

Where

- $B_\varepsilon(z,\rho) = \langle \varepsilon(r_1)\ \varepsilon(r_2) \rangle$ is the autocorrelation of permittivity fluctuations
- $\xi = \sigma_{Ne} / Ne$ and Ne is the electron density

- $A_{\xi}(\rho) = \int B_{\xi}(z, \rho)\, dz$
- ∇^2_{t1} , ∇^2_{t2} are the Laplacians with respect to r_1 and r_2 and $\rho = r_1 - r_2$

Equation (9) is a parabolic equation. It is two dimensions with respect to the distance and frequency separation. In the transform domain, it provides the medium scattering function dependency with respect to the Doppler frequency and delay. The algorithm developed uses again a multiple phase screen technique. In addition, if a quadratic approximation of the phase structure is used, which can be demonstrated whatever the medium spectrum slope value is, most of the calculations can be performed analytically [6].

Despite the fact that the Γ function depends on two variables, the Fourier transforms reduce to a one dimension FFT, the second transformation being done analytically. The result presented on Figure 5 has been obtained for HF propagation. A spread factor, named Q, related to the medium parameters can be defined and depending on its value, the shape of the scattering function may change significantly. The inhomogeneities sizes, the frequency and the distances have a strong influence on the signal spreading.

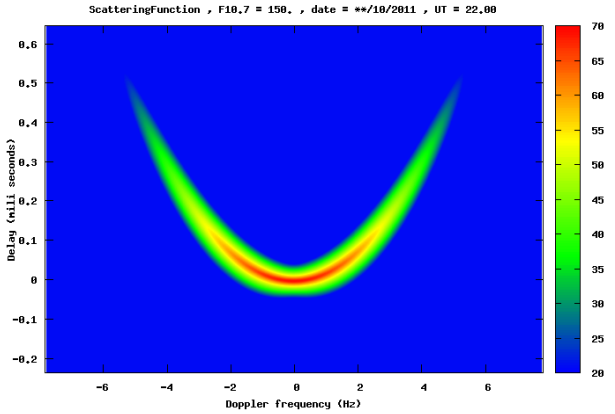

Figure 5: Mutual coherence function ; one single screen HF propagation (large Q value)

Solving equation (9) also provides the space, time and frequency coherence of the medium. The coherence time may be a limitation for Space Based Synthetic Aperture Radars (SAR), considering the satellite displacement velocity. On the contrary the frequency coherence is quite large and its decrease due to ionosphere turbulence appears to be less critical for most applications.

In the case of one single screen the whole calculation can be performed analytically. The solution is given by the expression below where S, B and P are functions of the phase variance, the frequency and the medium parameters as introduced by [7].

$$\Gamma(\tau, K_x, z) = \frac{z}{2\sqrt{SB}} \exp\left(-\frac{z^2 K_x^2}{4S}\right) \exp\left(-\frac{(\tau + z^2 K_x^2 P)^2}{4B}\right) \qquad (10)$$

with

$$B = \frac{\sigma_\Phi^2}{2\omega^2} \; ; \; S = \sigma_\Phi^2 L^2 \frac{\mathrm{Log}(L_0 / \ell_i)}{6\pi^2 L_0^2} \qquad (11)$$

and

$$P = \frac{1}{2 c k^2}\left(\frac{1}{z_{i+1}} - \frac{1}{z_i}\right) \qquad (12)$$

Where z_i is the coordinate along the propagation direction. This expression allows conducting a parametric analysis study.

4. Conclusion

The model presented in this paper, uses a classical phase screen technique algorithm. Sub models derived from previous measurement campaign results have been included to estimate some specific parameters and take the geophysical dependencies into account. When compared to measurements, the modeling results show a relatively good agreement as presented in section 2.5.

The last section is focused on the calculation of the transmitted field mutual coherence function. One analytical solution has been derived by assimilating the medium to one single phase screen. The characterization of this function is of particular interest for radar observations and remote sensing applications.

References

[1] Costa E., E. de Paula, L. Rezende, K. Groves, P. Roddy, E. Dao, M. Kelley, « Equatorial scintillation calculations based on coherent scatter radar and C/NOFS data, Radio Science, Vol **46**, doi :10.1029/2010RS004435, 2011

[2] Béniguel Y., P. Hamel, "A Global Ionosphere Scintillation Propagation Model for Equatorial Regions", Journal of Space Weather Space Climate, 1, (2011), doi: 10.1051/swsc/2011004

[3] Ishimaru A., Wave propagation and scattering in random media, Vol. **2**, Academic Press, ISBN 0-12-374702-3, 1978

[4] Rino C. L., A power law phase screen model for ionospheric scintillation, Radio Sci., Vol **14 (6)**, pp. 1135 – 1145, 1979.

[5] Béniguel Y., J-P Adam, N. Jakowski, T. Noack, V. Wilken, J-J Valette, M. Cueto, A. Bourdillon, P. Lassudrie-Duchesne, B. Arbesser-Rastburg, Analysis of scintillation recorded during the PRIS measurement campaign, Radio Sci., Vol 44, (2009), doi:10.1029/2008RS004090.

[6] Knepp D., L. J. Nickisch, Multiple phase screen calculation of wide bandwidth propagation, Radio Science, Vol **44**, doi:10.1029/2008RS004054, 2009

[7] Nickisch, L.J. Non uniform motion and extended media effects on the mutual coherence function: An analytic solution for spatial frequency, position and time, Radio Sc. Vol **27 (1)**, 1992